On the Need for Low Phase Noise Oscillators for Wireless Passive Sensor Probing

Nicolas Chrétien, Bruno François,
Gilles Martin, Sylvain Ballandras
FEMTO-ST, Time & frequency
32 avenue de l'observatoire
25044 Besançon, France
Emails: {nicolas.chretien,bruno.francois,
gilles.martin,ballandr}@femto-st.fr

Jean-Michel Friedt
SENSeOR, Besançon, France
Email: jmfriedt@femto-st.fr

Pratyush Varshney
Centre for Applied Research in Electronics
Indian Institute of Technology Delhi
Hauz Khas, New Delhi-110 016, India
Email: varshney.pratyush@gmail.com

***Abstract*—Two oscillators are needed for passive wireless sensor readers: a radiofrequency local oscillator generating the carrier within the bandpass of the sensor, and a clock triggering analog to digital conversion of the signals returned by the sensor. We assess the influence on measurement resolution of these two oscillators, hinting at some design rules of the sensor based on the characteristics of the oscillators as driven by cost, size, or power consumption. We demonstrate that local oscillator phase noise is a significant parameter in assessing the resolution of passive acoustic sensor probed through a wireless link, although with different characteristic conditions whether the sensor is in a delay line configuration (short term –far from carrier – response) or a resonator (long term – close to carrier – response).**

Keywords-surface acoustic wave; sensor; passive; wireless; phase noise; RADAR.

I. INTRODUCTION

Wireless passive sensors are either piezoelectric or dielectric transducers coupling with an incoming electromagnetic field following conditions dependent on the physical property under investigation. For instance, surface acoustic wave (SAW) delay lines convert an incoming electromagnetic pulse to a mechanical wave propagating on a piezoelectric substrate. Mirrors patterned on this substrate reflect a fraction of this wave back to the interdigitated transducer (IDT) connected to the antenna: the direct piezoelectric effect converts these acoustic pulses to electromagnetic signals detected by the receiver. Hence, a passive acoustic delay line reader operates following principles similar to RADAR, with a delayed echo not associated with reflections of the emitted signal over dielectric or conductive interfaces, but with delays associated with a measurement. Thus, all the well known RADAR techniques have been applied to passive wireless sensing, whether dielectric [1], [2], [3] or based on piezoelectric substrates [4], [5], [6], [7], [8], [9]: wideband pulsed RADAR [10], [11], FMCW RADAR [12], [13], FSCW RADAR [14], [8], [9], and chirped RADAR [15], [16].

Since it is well known that the local oscillator characteristics drives the detection capability of RADARs as will be discussed in the first introductory section of this presentation (Fig. 1), one might consider how local oscillator phase noise

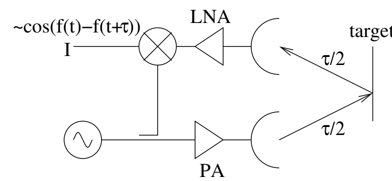

Figure 1. In case of a static target, a CW RADAR receiver noise detection limit is associated with the local oscillator frequency fluctuation between the emitted pulse at time t and the received pulse delayed by τ, the two-way transit duration.

affects passive wireless sensor resolution [17]. We extend in the third section the discussion from the classical passive target to the short-term – wideband – delay line acoustic sensor configuration in which the phase noise characteristics far from the carrier defines the measurement resolution. Since wideband acoustic delay lines are only compatible with the allocated 2.45 GHz band, we consider in the fourth section the same approach applied to narrowband resonators, compliant with the narrowband 434 MHz radiofrequency band, and the phase noise characteristics now shifted to the region close to the carrier. Such considerations will bring us in the fifth section to consider a second oscillator usually found on such circuits: the clock defining the analog to digital conversion rate. Thus, the reader is led throughout this paper to consider the various regions of the phase noise spectrum as a limiting factor for acoustic sensing resolution depending on the transducer characteristic time constants.

II. PHASE NOISE INFLUENCE ON CW RADAR

This introductory section reminds the reader of basic concepts related to phase noise of oscillators and their effect on RADAR detection capability. We will focus on the continuous wave (CW) RADAR where the explanation is straight forward.

CW RADARs are used whenever a velocity information is considered without ranging capability: a radiofrequency (RF) wave is generated by an oscillator. This signal is on the one hand fed to an antenna (after being amplified by a power amplifier, PA) and on the other hand a fraction of the output of the oscillator is sent to one input of a mixer. The second input of this mixer is fed with the signal detected by

 ISBN: 978-1-61208-208-0

either a second antenna in a bistatic configuration, or at the output of a circulator in a monostatic configuration, after amplification by a low noise amplifier (LNA). The output of the mixer m is the product of the frequency generated at time t by the oscillator but shifted by the Doppler frequency due to target motion δf, and the oscillator frequency delayed by a duration τ due to the electromagnetic wave propagation in air to and from the target:

$$\begin{aligned} m &= \cos\left(2\pi\left(f(t)+\delta f\right)\right) \times \cos\left(2\pi\left(f(t+\tau)\right)\right) \\ &\propto \cos\left(2\pi\left(f(t)+\delta f \pm f(t+\tau)\right)\right) \end{aligned} \qquad (1)$$

with only the difference term remaining after filtering the output by a low pass filter aimed at removing the signal at frequencies above f. Let us consider the case of slowly moving targets, where δf will be considered negligible; then $m \simeq \cos\left(2\pi\left(f(t)-f(t+\tau)\right)\right)$. Ideally this term should vanish when the target is not moving and assuming the oscillator ideally stable, *i.e.*, $f(t)$ constant; the only beat frequency would be associated to δf. However, oscillators do exhibit phase noise, and thus $f(t+\tau)$ and $f(t)$ differ: the phase noise spectrum of an oscillator is defined as the Fourier transform of the autocorrelation function of the oscillator output frequency [18].

The classical CW RADAR detection limit concludes that a moving target will only be detectable if its RADAR cross section is large enough so that the returned power (echo) is stronger than the power spectrum of the local oscillator: the phase variation is expressed in dBc/Hz, or a power with respect to the carrier power at an offset $1/\tau$ from the carrier frequency. As a concluding remark, long range RADAR is interested in the behavior of the oscillator close to the carrier (since $\tau = 2d/c$ with d the distance to the target and c the velocity of an electromagnetic wave: $d = 5-50$ km yields $\tau = 33-333$ μs in vacuum and thus the behavior of the oscillator at 3 to 33 kHz from the carrier is of interest). On the other hand, RADAR aimed at detecting moving walking people with targets in the sub-100 m range will only be affected by the phase noise above 1.5 MHz from the carrier.

III. Application to SAW reflective delay line sensing

One implementation of SAW delay line readers acts exactly as a CW reader: a carrier is chopped in pulses containing as many periods as there are electrodes in the sensor IDT (Fig. 2).

The reader on the one hand emits these pulses whose frequency is centered on the oscillator frequency output, and the returned signal from the sensor is centered on the same frequency, but shifted in time by a duration dependent on the physical property under investigation (which most significantly affects the acoustic wave velocity on the piezoelectric substrate). Thus, the mixer output exhibits a series of pulses whose rough delay is estimated through maximum returned power (threshold) or cross-correlation; but it is well

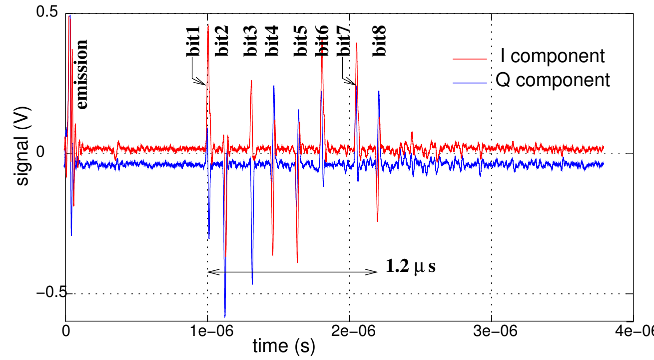

Figure 2. Typical response from a SAW delay line, here from a temperature sensor with 8-bit coding sold by CTR Carinthian Tech Research (Villach, Austria), here excited by a 40-ns long pulse centered on 2.40 GHz. The pulse at 0 s is the excitation pulse, and the returned echos are located between 1 and 2.2 μs.

known that only a phase measurement (with 2π uncertainty) provides the required high accuracy on the acoustic velocity and thus the measured physical quantity [19], [20].

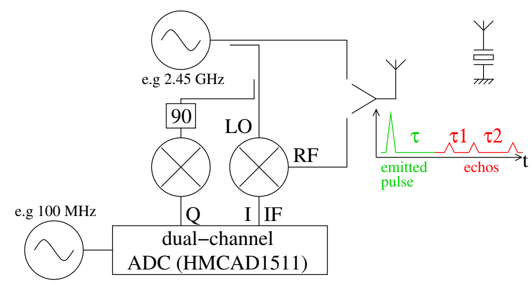

Figure 3. Demodulation circuit for probing wireless passive SAW sensors. The mixer might be replaced by an I/Q demodulator in practical systems.

Let us now add to the time delay from the acoustic wave propagation another contribution to the detected phase: the local oscillator intrinsic noise as characterized by its phase noise. The phase noise of a signal $V(t) = (V_0+\varepsilon(t))\sin\left(2\pi f_0 t + \Delta\varphi(t)\right)$ is defined as [21] the phase fluctuations in a 1 Hz-wide bandwidth

$$S_{\Delta\varphi} = \frac{\Delta\varphi^2_{RMS}}{\text{measurement bandwidth}} \ \text{rad}^2\text{/Hz}$$

and the classical representation of the noise spectrum is given by $L(f) = \frac{1}{2}S_{\Delta\varphi}(f) = 10 \times \log_{10}\left(\frac{P_{SSB}}{P_S}\right)$ dBc/Hz.

Based on these informations, we will compute the phase noise fluctuations of the local oscillators during time intervals τ which are now given by the travel duration of the electromagnetic wave in the medium surrounding the sensor (negligible since readout ranges are in the tens of meters at most, or tens of nanoseconds) and the acoustic delay which is typically in the 1 to 5 μs range: the offset to the carrier of interest to acoustic sensing is in the 200 kHz to 1 MHz range.

This frequency range usually lies above the Leeson frequency $f_L = f_{LO}/(2Q_{LO})$ with f_{LO} and Q_{LO} the

 ISBN: 978-1-61208-208-0

local oscillator resonator frequency and quality factor. This characteristic frequency defines a frequency offset from the carrier at which the resonator no longer acts as an energy tank and becomes transparent to the feedback amplifier noise. Above this frequency, the phase noise of the oscillator is constant and solely defined by the power injected in the resonator, the noise factor of the feedback amplifier and the operating temperature. We shall come back to such considerations in the design section.

Two practical applications will focus on a poor oscillator assumed to exhibit -130 dBc/Hz, and an excellent oscillator assumed to exhibit -170 dBc/Hz as the frequency offset of interest. Another numerical application using -90 dBc/Hz is justified by the fact that the returned signal noise floor is the maximum of either the initial oscillator noise floor raised by the power amplifier (PA) and low noise amplifier (LNA), or the LNA noise floor set by its thermal noise $F_{LNA}k_BT/P_R$ with $F_{LNA} \simeq 1.5$ dB the noise factor of the reception amplifier, $10\log_{10}(k_BT) = -174\ dBm$ the product of the Boltzmann constant with the temperature $T = 290$ K, and P_R the received power. From this consideration, the measurement resolution will first be constant as long as the LNA noise floor is lower than the LO noise floor, and drops once the returned power becomes so low that the LNA noise floor rises above the LO noise floor. The received power is related to the emitted power P_E – limited to $P_E = +10$ dBm by radiofrequency emission regulations in 434 and 2450 MHz ISM bands – through the free space propagation losses and the sensor insertion losses. Free space propagation losses $FSPL = \left(\frac{4\pi df}{c}\right)$ are associated with energy distribution on a sphere generated by the emitter, and in the case of a RADAR the link budget requires the use of $FSPL^4$ since the target itself acts as a point-like source generating a spherical wave. The SAW sensor insertion loss IL is a significant source of energy loss when probing SAW delay lines since a typical IL value is -35 dB. Thus, $P_R = P_E \times FSPL^4 \times IL$ and switching to a logarithmic description, the noise floor on the return branch reaching the mixer is either the floor of the oscillator raised by the noise floor of PA and LNA, or the noise floor of the LNA amplifier $F_{LNA,dB} + 10\log_{10}(k_BT) - 10\log_{10}(P_E \times FSPL^4) - IL)$. The lower the oscillator phase noise floor, the smaller the range at which the LNA noise floor becomes dominant, as shown in the numerical application of Table I.

In such cases, the phase variations due to the local oscillator are $\Delta\varphi_{RMS} = \sqrt{2 \times 10^{-(130..170)/10}}$ rad/$\sqrt{\text{Hz}}$. Since we focus on measuring the phase within a 30 ns long pulse, the measurement bandwidth is 60 MHz and $\Delta\varphi_{RMS} = \sqrt{2 \times 10^{-(130..170)/10} \times 60 \times 10^6}$ rad whose numerical application yields to phase fluctuations from 0.2^o to 0.002^o (for -130 and -170 dBc/Hz cases respectively).

We must now relate these phase fluctuations with the phase variations due to a physical quantity variation: we

Operating freq.	osc. noise floor	distance
100 MHz	-170 dBc/Hz	0.04 m
100 MHz	-130 dBc/Hz	0.4 m
100 MHz	-90 dBc/Hz	4.2 m
2450 MHz	-170 dBc/Hz	0.002 m
2450 MHz	-130 dBc/Hz	0.02 m
2450 MHz	-90 dBc/Hz	0.2 m

Table I
DISTANCE AT WHICH THE LNA NOISE FLOOR REACHES THE LOCAL OSCILLATOR NOISE FLOOR, THUS BECOMING DOMINANT AT THE MIXER OUTPUT.

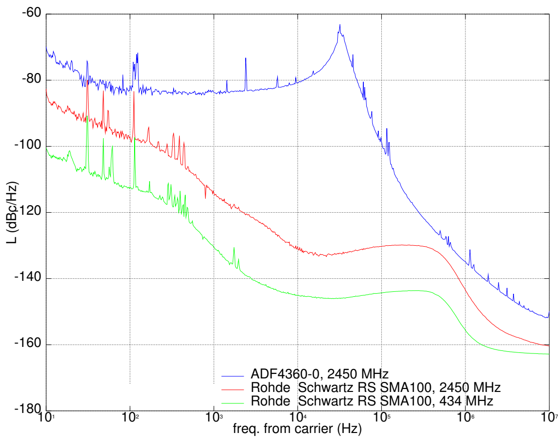

Figure 4. Phase noise of a 2.45 GHz source generated by an Analog Devices ADF4360-0 Phase Locked Loop (poorly controlled), and Rohde & Schwartz SMA 100A tabletop frequency synthesizer set to 2450 and 434 MHz.

focus on a temperature sensor. An acoustic sensor exhibits a phase rotation for every period, *i.e.*, for a propagation length of one wavelength λ. The elastic wave propagates on the piezoelectric substrate at velocity v and the time-difference due to the two-way trip d from IDT to the mirror yields a phase shift of

$$\Delta\varphi = 2\pi \times d/\lambda = 2\pi \times d \times f/v$$

The variation with temperature T of this phase difference is associated with the velocity variation, so that

$$\left.\frac{\partial\Delta\varphi}{\Delta\varphi}\right|_T = \left.\frac{\partial v}{v}\right|_T \Leftrightarrow \partial\Delta\varphi(T) = 2\pi\frac{d \times f}{v} \times \left.\frac{\partial v}{v}\right|_T$$

All quantities in this equation are known: for a $LiNbO_3$ substrate, we consider that $v \simeq 3000$ m/s, $\partial v/v \simeq 60$ ppm/K. Selecting $d = 10$ mm and $f = 100$ MHz (as used in [22]), we conclude that $2\pi \times 60 \times 10^{-6} \times 10^{-2} \times 10^8/3000 = 0.13$ rad/K= 7.2 ^{o}/K.

By extending this analysis to various experimental parameters, we compare the local oscillator phase noise fluctuation implication on the measurement resolution in Table II.

We conclude that the local oscillator stability becomes a significant hindrance to high resolution temperature measurements, and reaching the mK resolution as was done

ISBN: 978-1-61208-208-0

Phase noise	half distance between reflectors	resolution
-170 dBc/Hz	10 mm	2×10^{-4} K
-170 dBc/Hz	1 mm	2×10^{-3} K
-130 dBc/Hz	10 mm	0.02 K
-130 dBc/Hz	1 mm	0.2 K
-90 dBc/Hz	10 mm	2 K
-90 dBc/Hz	1 mm	20 K

Table II
TEMPERATURE MEASUREMENT RESOLUTION, ASSUMING A 60 PPM/K TEMPERATURE DRIFT OF THE DELAY-LINE SENSOR, AS A FUNCTION OF VARIOUS LOCAL OSCILLATOR PARAMETERS.

with the Hewlett Packard HP2830A resonator-based probes is challenging.

Beyond the compliance with radiofrequency emission regulations, the use of ultra-wideband (UWB) interrogation strategies, *e.g.*, Ground Penetrating RADAR based approaches [22], yields the question of optimum operating frequencies. Indeed, we have seen that the time delay is a function of the acoustic velocity and propagation path length (defined respectively by selecting appropriate single-crystal piezoelectric substrate orientations, and design considerations in positioning the mirrors on the sensor surface), but also of the operating frequency:

$$\Delta\varphi = 2\pi d/\lambda = 2\pi df/v = 2\pi f\tau$$

where τ is the propagation duration of the pulse, *i.e.*, $\partial\Delta\varphi = 2\pi f\partial\tau \Leftrightarrow \partial\tau = 1/(2\pi f)\partial\Delta\varphi$, providing the relationship between phase noise and delay noise through the inverse of the frequency.

The remaning design issue lies in the selection of the echo pair used for computing acoustic propagation time delay and thus identifying the physical quantity under investigation. The first and last echos of a tag (start and stop bits) are usually considered for such purposes. However, the further away mirrors are, the longer the delay and thus the larger the local oscillator fluctuations, associated with phase noise rise. One should thus take care that the inverse of the propagation delay does not reach the Leeson frequency f_L where the noise floor meets the rising phase noise slope: $f_L = f_0/(2Q)$. Considering a (very favorable) $Q = 20000$ resonator used for generating a 2.45 GHz oscillator, $f_L =$ 60 kHz and the associated propagation delay is 16 μs, far above any practical limitation (such a delay would be associated with a 24 mm-long propagation path). However, for a more reasonable $Q = 2000$ [23], the Leeson frequency reaches 600 kHz or a propagation delay of 1.6 μs. In this case, using echos returned by mirror at extreme positions of the delay line should be avoided (*i.e.*, exhibiting propagation delays larger than 1.6 μs) and adjacent echos should yield results with higher resolutions.

IV. SENSOR DESIGN WITH RESPECT TO LOCAL OSCILLATOR CHARACTERISTICS

Consider two applications: a 434 MHz delay line (which would not comply with RF regulations) and a 2450 MHz delay line. Resonators in the former frequency range exhibit typical quality factors of 10000, and $f_L = 22$ kHz, well below the 200-1000 kHz range we have been considering: a classical delay line design will be probed at best by the reader. However at 2450 MHz, since the product $Q \times f$ is constant for a given technology, the local oscillator Q drops to 1800, and the Leeson frequency rises to 680 kHz. The designer of a 2450 MHz delay line would be wise to avoid the phase noise rise below f_L and limit the maximum time delay on the acoustic path to 1.5 μs. Since electromagnetic clutter fades within the first 700 ns (assuming 100 m range) and the typical pulse length is 40 ns spaced by at least 100 ns to account for manufacturing variability, limiting the delay to 1.5 μs still leaves enough space for 5 reflections, more than enough for multi-parameter-sensing (one reference pulse and 4 pulses for probing 4 different physical quantities, *e.g.*, temperature [24], pressure [25] and two chemical compounds [26].

V. APPLICATION TO SAW RESONATOR SENSING

SAW resonator probing aims at identifying a characteristic frequency: in one embodiment of this approach, a frequency sweep network analyzer sequentially probes multiple frequencies in order to identify the frequency at which the sensor returns a maximum power. SAW resonators store energy during the electromagnetic signal emission phase, and release this energy (as an electromagnetic wave at the sensor resonance frequency f_0) during the listening stage: the time constant of each step is $Q/(\pi f_0)$ with Q the sensor quality factor. The fastest approach to the best of our knowledge [27] for probing a resonance frequency of a resonator requires two signals at different frequencies, one above and one below f_0 (Fig. 5).

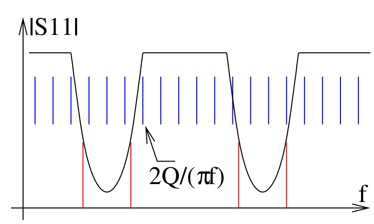

Figure 5. For a dual-mode resonator, required for a differential measurement, a minimum of 4 measurements each lasting $2Q/(\pi f)$ seconds, with f the resonance frequency of one mode and Q its quality factor, is needed (red). A more classical approach of a frequency sweep network analyzer requires up to 128 measurements in the 434-MHz European ISM band (blue).

Hence, the minimum measurement duration is $2Q/(\pi f_0)$ for each probed frequency. For $f_0 = 434$ MHz and $Q =$ 10000 in a dual resonator configuration, eight time constants (two resonators, and for earch two-measurement points, and for each one time constant for loading and unloading the resonator) yield 59 μs measurement duration, so that the oscillator stability at 17 kHz from the carrier is of interest.

Phase noise	frequency	Q	$\Delta f_{RMS}(Hz)$	resolution
-170 dBc/Hz	434 MHz	10000	0.01	4.10^{-7} K
-130 dBc/Hz	434 MHz	10000	1	4.10^{-5} K
-90 dBc/Hz	434 MHz	10000	140	5 mK
-170 dBc/Hz	2.450 GHz	1500	2	10^{-5} K
-130 dBc/Hz	2.450 GHz	1500	230	1 mK
-90 dBc/Hz	2.450 GHz	1500	23000	0.1 K

Table III
FREQUENCY STANDARD DEVIATION AS A FUNCTION OF THE CHARACTERISTICS OF THE RESONATOR USED AS SENSOR (DEFINING THE TIME CONSTANT OF THE INTERROGATION).

The phase noise $S_{\Delta\varphi}$ and frequency noise (or stability) $S_{\Delta f}$ at f from the carrier are related through

$$S_{\Delta f} = f^2 \times S_{\Delta\varphi} = \frac{\Delta f_{RMS}^2}{BW}$$

So, with a measurement bandwidth BW of $2f$, frequency fluctuations are given by

$$\Delta f_{RMS} = \sqrt{BW \times f^2 \times 2L(f)}$$

The result of this calculation is summarized in table III, assuming that the $Q \times f$ product is constant, as is usually considered for a given technology, with values representative of SAW resonators patterned on a quartz substrate. The temperature resolution – last column of Table III – is computed assuming a 60 ppm/K sensitivity. This last result scales as the temperature sensitivity of the substrate: a sensor allowing for a 170 K measurement range within the 1.7 MHz wide 434 MHz European ISM band – as sold by SENSeOR (Mougins, France) – only exhibits a 5.7 ppm/K sensitivity and hence the values in the last column are multiplied by 10.

Here again, for resonators acting as temperature sensors with 2.5 kHz/K temperature sensitivity (in order to fit a 170 K measurement range within the 1.7 MHz wide 434 MHz Industrial, Scientific and Medical (ISM) band, accounting for manufacturing variations), the 25 Hz frequency resolution (10 mK resolution) is only met if a reasonably stable local oscillator is used as reference, with a phase noise below -105 dBc/Hz. This result is consistent with the phase noise spectra provided in [28], with a phase noise around -105 dBc/Hz in the 500-5000 Hz carrier offset range at the 434 MHz DDS output. The former range boundary is met when probing 128-samples in a frequency-sweep network analyzer approach: 128 points each requiring $2Q/(\pi f_0)$ requires a duration of 1.8 ms or an update rate of 530 Hz.

VI. ANALOG TO DIGITAL CONVERSION JITTER

We now change oscillator type to consider the analog to digital conversion (ADC) stage. The phase measurement requires two simultaneous measurements of the I and Q components of the returned signal after mixing with the local RF oscillator. The typical pulse duration is 30 ns so that the ADC bandwidth must be at least in the $f_s = 60$ MHz range, or practically (3 points/period at least) 100 MHz.

Measuring a phase with 0.13 rad resolution over the full 2π range requires $bits = 6$ bit resolution. Since the jitter on the clock controlling the ADC yields a resolution loss (linear scale) of $SNR = (2\pi f_s \sigma_t)$, the jitter σ_t must not exceed

$$\sigma_t \leq 2^{-bits}/(2\pi \times f_s)$$

which is here equal to 42 ps [29]. However, increasing 10-fold this resolution yields a 9 bit ADC resolution and a maximum jitter of 5 ps.

On the other hand, let us estimate the jitter induced by an oscillator exhibiting a -130 dBc/Hz phase noise level in the 200 kHz-200 MHz range, representative of the influence of the clock controlling the ADC sampling at 100 MS/s for a maximum duration of 5 μs. The RMS jitter (in seconds) is given [30] by

$$\sigma_t = \frac{\sqrt{2 \times 10^{-130/10} \times 10^8}}{(2\pi \times 10^8)}$$

which is equal to 7 ps, dropping the lower integration limit (200 kHz) by assuming that the constant phase noise level extends to the carrier. Thus, although even a very poor reference oscillator controlling the ADC meets the requirements of 9-bit resolution needed for high resolution temperature measurements, care should nevertheless be taken to reach sub-10 ps jitter. As an example, the Digital PLL generating the clock output of an iMX27 CPU as used on the APF27-board from Armadeus Systems (Mulhouse, France) for prototyping our experiments is specified at a maximum of 200 ps, hardly usable for the application described here [31].

VII. CONCLUSION

While the debate on the advantages between delay line and resonator approaches is still ongoing, local oscillator characteristics brings some hint on which strategy might bring the most accurate result. From a local oscillator perspective, moving the frequency offset as far as possible from the carrier, *i.e.*, allowing for as short a duration between various measurements of the sensor characteristics as possible, clearly hints at an advantage towards delay lines. However, this partial picture does not include the receiver noise level, especially the high bandwidth on the ADC sampling required to recover and digitize the fast delay line response: only an extremely stable (low jitter) clocking circuit for the receiver ADC will provide measurements with resolutions comparable to those of resonators. Furthermore, as opposed to FMCW or frequency sweep approaches which require tunable frequency sources (VCO, frac-PLL, DDS), a pulsed (UWB-like) delay line approach only requires a *fixed frequency* source generating a stable signal within the bandpass of the sensor, hence allowing for improved stability. Such results are most significantly the target of high quality factor piezoelectric resonator based oscillators aimed at reaching the targetted radiofrequency band.

Design rules concerning the oscillator characteristics are provided for delay lines: the maximum two-way trip duration should be lower than the inverse of the Leeson frequency, while only low noise floor enables high resolution measurements as explicitly stated with relationships between local oscillator phase noise densities and measured returned signal phase resolution. For resonator probed through a frequency sweep network analyzer approach, the tunable local oscillator source is clearly a limiting factor in the measured resonance frequency resolution.

REFERENCES

[1] C. Allen, K. Shi, and R. Plumb, "The use of ground-penetrating radar with a cooperative target," *IEEE Transactions on Geoscience and Remote Sensing*, vol. 5, no. 2, pp. 1821–1825, 36 1998.

[2] V. Sridhar and K. Takahata, "A hydrogel-based passive wireless sensor using a flex-circuit inductive transducer," *Sensors and Actuators A: Physical*, vol. 155, no. 1, pp. 58–65, 2009.

[3] M. Jatlaoui, F. Chebila, S. Bouaziz, P. Pons, and H. Aubert, "Original identification technique of passive em sensors using loaded transmission delay lines," in *European Microwave Conference (EuMC)*, Sept. 2010, pp. 1106–1109.

[4] A. Pohl, F. Seifert, L. Reindl, G. Scholl, T. Ostertag, and W. Pietsch, "Radio signals for SAW ID tags and sensors in strong electromagnetic interference," in *IEEE Ultrasonics Symposium*, Cannes, France, 1994, pp. 195–198.

[5] L. Reindl, G. Scholl, T. Ostertag, C. Ruppel, W.-E. Bulst, and F. Seifert, "SAW devices as wireless passive sensors," in *IEEE Ultrasonics Symposium*, 1996, pp. 363–367.

[6] W. Bulst, G. Fischerauer, and L. Reindl, "State of the art in wireless sensing with surface acoustic waves," *IEEE Transactions on Industrial Electronics*, vol. 48, no. 2, pp. 265–271, April 2001.

[7] A. Stelzer, R. Hauser, L. Reindl, and R. Teichmann, "A low-cost interrogation unit and signal processing for a SAW identification-tag for a pressure sensor," in *XVII IMEKO World Congress*, June 2003, pp. 672–675.

[8] G. Bruckner, A. Stelzer, L. Maurer, J. Biniasch, L. Reindl, R. Teichmann, and R. Hauser, "A high-temperature stable SAW identification tag for a pressure sensor and a low-cost interrogation unit," in *11th International Sensor Congress (SENSOR)*, Nuremberg, Germany, 2003, pp. 467–472. [Online]. Available: http://www.rfid.co.uk/knowledge_centre/pdfs/hightemprfid.pdf

[9] S. Schuster, S. Scheiblhofer, L. Reindl, and A. Stelzer, "Performance evaluation of algorithms for SAW-based temperature measurement," *IEEE Transactions on Utrasonics, Ferroelectrics, and Frequency Control*, vol. 53, no. 6, pp. 1177–1185, june 2006.

[10] Y. Wen, P. Li, J. Yang, and M. Zheng, "Detecting and evaluating the signals of wirelessly interrogational passive SAW resonator sensors," *IEEE Sensors journal*, vol. 4, no. 6, December 2004.

[11] M. Hamsch, R. Hoffmann, W. Buff, M. Binhack, and S. Klett, "An interrogation unit for passive wireless SAW sensors based on Fourier transform," *IEEE Transactions on Ultrasonics, Ferroelectrics, and Frequency Control*, vol. 51, no. 11, pp. 1449–1456, November 2004.

[12] A. Stelzer, G. Schimetta, L. Reindl, A. Springer, and R. Weigel, "Wireless SAW sensors for surface and subsurface sensing applications," in *SPIE Proceedings – Subsurface ans Surface Sensing Technologies and Applications III*, vol. 4491, 2001, pp. 358–366.

[13] J. Beckley, V. Kalinin, M. Lee, and K. Voliansky, "Non-contact torque senseor based on SAW resonators," in *IEEE Int. Freq. Control Symposium and PDA Exhibition*, New Orleans, LA, USA, 2002, pp. 202–213.

[14] G. Scholl, F. Schmidt, T. Ostertag, L. Reindl, H. Scherr, and U. Wolff, "Wireless passive SAW sensor systems for industrial and domestic applications," in *IEEE International Frequency Control Symposium*, 1998, pp. 595–601.

[15] A. Springer, M. Huemer, L. Reindl, C. W. Ruppel, A. Pohl, F. Seifert, W. Gugler, and R. Weigel, "A robust ultra-broad-band wireless communication system using SAW chirped delay lines," *IEEE Transactions on Microwave Theory and Techniques*, vol. 46, no. 12, pp. 745–756, december 1998.

[16] D. Puccio, D. Malocha, D.Gallagher, and J.Hines, "SAW sensors using orthogonal frequency coding," in *IEEE Frequency Control Symposium*, 2004, pp. 307–310.

[17] V. Kalinin, "Influence of receiver noise properties on resolution of passive wireless resonant SAW sensors," in *IEEE Ultrasonics Symposium*, vol. 3, 2005, pp. 1452–1455.

[18] E. Rubiola, *Phase Noise and Frequency Stability in Oscillators*. Cambridge University Press, 2010.

[19] J. H. Kuypers, M. Esashi, D. A. Eisele, and L. M. Reindl, "2.45 GHz passive wireless temperature monitoring system featuring parallel sensor interrogation and resolution evaluation," in *IEEE Ultrasonics Symposium*, 2006, pp. 1453–1458.

[20] L. Reindl, "Wireless passive SAW identification marks and sensors," *2nd Int. Symp. Acoustic Wave Devices for Future Mobile Communication Systems*, pp. 1–15, March 2004.

[21] "Phase noise characterization of microwave oscillators – phase detector method," *Agilent Product Note*, vol. 11729B-1.

[22] J.-M. Friedt, T. Rétornaz, S. Alzuaga, T. Baron, G. Martin, T. Laroche, S. Ballandras, M. Griselin, and J.-P. Simonnet, "Surface acoustic wave devices as passive buried sensors," *Journal of Applied Physics*, vol. 109, no. 3, p. 034905, 2011.

[23] U. Knauer, J. Machui, and C. Ruppel, "Design, fabrication, and application of GHz SAW devices," in *Microwave Symposium Digest – IEEE MTT-S International*, vol. 3, 1997, pp. 1821–1824.

[24] R. Fachberger, G. Bruckner, R. Hauser, and L. Reindl, "Wireless SAW based high-temperature measurement systems," in *IEEE International Frequency Control Symposium and Exposition*, 2006, pp. 358–367.

[25] W. Buff, M. Rusko, M. Goroll, J. Ehrenpfordt, and T. Vandahl, “Universal pressure and temperature SAW sensor for wireless applications,” in *IEEE Ultrasonics Symposium*, 1997, pp. 359–362.

[26] Y. Dong, W. Cheng, S. Wang, Y. Li, and G. Feng, “A multi-resolution passive SAW chemical sensor,” *Sensors and Actuators B*, vol. 76, pp. 130–133, 2001.

[27] J.-M. Friedt, C. Droit, S. Ballandras, S. Alzuaga, G. Martin, and P. Sandoz, “Remote vibration measurement: a wireless passive surface acoustic wave resonator fast probing strategy,” *Rev. Sci. Instrum.*, vol. 83, p. 055001, 2012.

[28] J.-M. Friedt, C. Droit, G. Martin, and S. Ballandras, “A wireless interrogation system exploiting narrowband acoustic resonator for remote physical quantity measurement,” *Rev. Sci. Instrum.*, vol. 81, p. 014701, 2010.

[29] D. Redmayne, E. Trelewicz, and A. Smith, “Understanding the effect of clock jitter on high speed ADCs,” available at cds.linear.com/docs/Design%20Note/dn1013f.pdf, last accessed 08/08/2012, 2006.

[30] W. Kester, “Converting oscillator phase noise to time jitter,” available at http://www.analog.com/static/imported-files/tutorials/MT-008.pdf, last accessed 08/08/2012, 2008.

[31] “i.MX27 and i.MX27L data sheet,” available at www.freescale.com/files/dsp/doc/data_sheet/MCIMX27EC.pdf, last accessed 08/08/2012, 2011.